

Intelligent Energy Optimizer for Residential Buildings



Niraj Kunwar
Mahabir Bhandari
Kuldeep Kurte
Anthony Gehl
Bipin Shah*
Logesh Janarthanan*

**CRADA final report for
CRADA number NFE-21-08439**

*Winbuild Inc.

October 2022



DOCUMENT AVAILABILITY

Reports produced after January 1, 1996, are generally available free via OSTI.GOV.

Website www.osti.gov

Reports produced before January 1, 1996, may be purchased by members of the public from the following source:

National Technical Information Service

5285 Port Royal Road

Springfield, VA 22161

Telephone 703-605-6000 (1-800-553-6847)

TDD 703-487-4639

Fax 703-605-6900

E-mail info@ntis.gov

Website <http://classic.ntis.gov/>

Reports are available to US Department of Energy (DOE) employees, DOE contractors, Energy Technology Data Exchange representatives, and International Nuclear Information System representatives from the following source:

Office of Scientific and Technical Information

PO Box 62

Oak Ridge, TN 37831

Telephone 865-576-8401

Fax 865-576-5728

E-mail reports@osti.gov

Website <https://www.osti.gov/>

Buildings and Transportation Science Division

INTELLIGENT ENERGY OPTIMIZER FOR RESIDENTIAL BUILDINGS

Niraj Kunwar

Mahabir Bhandari

Kuldeep Kurte

Anthony Gehl

Bipin Shah*

Logesh Janarthanan*

October 2022

Prepared by
OAK RIDGE NATIONAL LABORATORY
Oak Ridge, TN 37831
managed by
UT-BATTELLE LLC
for the
US DEPARTMENT OF ENERGY
under contract DE-AC05-00OR22725

CONTENTS

LIST OF FIGURES	vi
LIST OF TABLES	vi
ABSTRACT.....	7
ACKNOWLEDGEMENTS	8
1. INTRODUCTION	9
2. METHODOLOGY AND RESULTS.....	10
2.1 DATA COLLECTION	11
2.2 EVENT DETECTION	11
2.2.1 Step 1: Always-On Component	11
2.2.2 Step 2: Smoothing.....	12
2.2.3 Step 3: Event Detection	12
2.3 EVENT CLASSIFICATION	13
2.3.1 K-Means Clustering	13
2.3.2 RBC	17
3. CONCLUSIONS.....	22
4. REFERENCES	22

LIST OF FIGURES

Figure 1. Time series of the raw active power signal and preprocessed data.	12
Figure 2. Time series of raw active power and events detected using preprocessed data.....	13
Figure 3. Plot of number of clusters vs. inertia.	14
Figure 4. Clustering of equipment start events: iteration 1.....	15
Figure 5. Clustering of equipment start events: iteration 2.....	16
Figure 6. Bounding boxes for classification of different appliances.	18
Figure 7. Bounding boxes for classification with scatter plot of transient-state 95th percentile power against steady-state median values obtained from individual power data of appliances.	19
Figure 8. Bounding boxes for classification with scatter plots of transient-state 95th percentile power against steady-state median power obtained from disaggregation of mains electricity.	19

LIST OF TABLES

Table 1. Appliance that had start event when a start event was detected in mains.....	17
Table 2. Cross-table of classification of appliances using RBC using active power vs. event detected using individual appliance power	20
Table 3. Cross-table of classification of appliances using RBC using reactive power vs. event detected using individual appliance power	20
Table 4. Appliance classification metrics using active power	22
Table 5. Appliance classification metrics using reactive power	22

ABSTRACT

Demand-side management in the buildings is essential for meeting grid flexibility needs in a highly renewable energy scenario. Appliance load monitoring helps decision making for demand-side management by providing the information on operation status/power consumption from different appliances in the buildings. Nonintrusive load monitoring (NILM) is an attractive option for appliance load monitoring using because it has lower cost for sensors and helps mitigate privacy concerns. In this study, the team used an event detection technique followed by two different methods for event classification. The results from k-means clustering showed that the events from a single appliance are often distributed in multiple clusters. Thus, the unsupervised method of NILM using k-means clustering used in this study was not very suitable for load disaggregation. The results from NILM showed that the F1-score for event classification was 0.77 for a heat pump water heater and very low for other appliances using the rule-based classification.

ACKNOWLEDGEMENTS

We would like to thank Erika Gupta at the US Department of Energy for guiding this research.

1. INTRODUCTION

Buildings consume approximately 75% of electricity in the United States (“US Energy Information Administration” 2019). The strategic goal of the US Department of State is to achieve net-zero greenhouse gas emissions by 2050, and clean distributed energy sources (including solar and wind) would be used for electricity production (United States Department of State 2021). However, because of the intermittent nature of renewable energy generation, energy storage and demand-side management are critical for meeting grid flexibility needs (Langevin et al. 2021). As the largest consumer of electricity, buildings are the major sector for providing demand-side management. *Demand-side management* refers to the change in electric energy consumption (load shape) by the end users to meet the needs of the electric grid (Gelazanskas and Gamage 2014). Various technologies and systems should be developed or upgraded for reliable and efficient demand-side management, including advanced metering infrastructures, controllers, and communication systems for enabling effective decision making (Siano 2014). Load monitoring is an essential component of demand-side management since it provides information of the operation status of various appliances in a building. The appliance load monitoring can be performed in both intrusive and nonintrusive techniques. Intrusive monitoring, however, requires costly submeter installations and raises privacy concerns (Hosseini et al. 2017). These issues have resulted in significant research efforts toward nonintrusive load monitoring (NILM), which was introduced three decades ago by George Hart (Hart 1992). NILM includes analysis of voltage, current, and their derivatives of total load to predict the number, nature, and operation and energy consumption of individual loads.

The main steps for NILM include data collection, event detection, feature extraction, and load identification (Ruano et al. 2019). Data collection for NILM varies from sub-hourly data (Parson et al. 2016) to high-frequency data in kilohertz (Filip 2011). The duration of the data collection (a few days to multiple years) and the number of buildings (one to hundreds) for which data are available also widely vary (Faustine et al. 2017). NILM can be used to detect on/off events of the appliance as a classification problem or predict the energy consumption by the appliances as a regression problem. Different methods, such as event-based methods that use a change detection algorithm or state-based methods that use probability distribution/optimization, have been used for NILM (Le and Kim 2018). However, most of the prior NILM techniques used cannot perform disaggregation in real-time (Faustine et al. 2017). In this study, the team investigated an event detection-based algorithm that has potential to classify events in near real-time.

Winbuild Inc.’s technology is an intelligent energy optimizer based on principles of power optimization. It senses the building load and matches that with the source impedance. The power optimization system measures load parameters, including voltage, power factor, harmonics, reactive power, and maximum

demand, and automatically senses the necessity for voltage optimization, reactive power compensation, and harmonic suppression. The power optimization system constantly senses the incoming voltage and optimizes and maintains it within a specific rated voltage range. This setup has greater potential for load savings during loading/unloading and switching on/off of an inductive load. The system also keeps the power factor close to unity, and harmonics are suppressed. The power optimizer also has an integrated remote load management functionality. The product has been tested for residential applications. Based on user feedback, Winbuild is enhancing the system that can group the load based on the usage pattern, which can help users to understand and take further measures on energy savings. Furthermore, predicting the connected load/equipment efficiency will help preventive maintenance by reducing maintenance costs and unscheduled shutdowns.

In this project, the team utilized NILM to obtain information on usage patterns of different appliances based on measurement of electric signals input in a subpanel. The initial main assumption for NILM in this project was that the information on the individual appliance operation will not be available for training purposes. This assumption included the absence of any information on electricity data of individual appliances, the number of appliances present in the building, or the types of appliances present in the building. The main reason for this approach was to create a generic method that could be applied to any residential building for NILM. Thus, only the main data would be used for NILM, and individual data could be used to verify the accuracy of NILM. Under this approach, the work described in Sections 2.1–2.3.1 was performed. However, seeing the limitation of this approach to categorize any appliance, Section 2.3.2 describes efforts in which the individual appliance data were used for event classification. Thus, the team explored unsupervised learning using k-means clustering of the signal during a start event, as well as a rule-based classification (RBC) based on the appliance signal during a transient period and steady-state period.

2. METHODOLOGY AND RESULTS

The electricity data were collected for a subpanel located in the garage of the Yarnell Station research house, which is a residential test facility at the US Department of Energy's Oak Ridge National Laboratory. For NILM, the monitoring was performed in two steps: event detection and event classification.

2.1 DATA COLLECTION

The data were collected for incoming electricity at the subpanel, as well as different appliances connected to the subpanel, which were as follows:

- HVAC: outdoor unit (OD) and indoor unit (ID)
- Heat pump water heater (HPWH)
- Dryer
- Fridge
- Microwave

The house is an unoccupied house where the occupant load is simulated, so dryer and microwave were only run for a couple of days, and the majority of the data collected included the cycles for the HVAC system and HPWH. The data were collected for approximately 1.5 months, which included current, voltage, active power, and apparent power data. The data were collected at 1 s intervals for each of the appliances, as well as total subpanel electricity (i.e., mains data).

2.2 EVENT DETECTION

An event detection algorithm was used on the mains data. Before event detection, the mains data were preprocessed via the method used by Patten (Patten 2012). Preprocessing of the data involved disaggregating the electricity consumption to an always-on component and variable component. Here, $\{x: x_1, x_2, \dots, x_n\}$ is the time series representing the electrical mains data ; the steps used for preprocessing and event detection following (Patten 2012) are discussed next.

2.2.1 Step 1: Always-On Component

The always-on threshold (ao_{th}) is defined as

$$ao_{th} = 0.5 \text{ percentile of elements in } x . \quad (1)$$

The always-on component (aoc_x) and variable component (vc_x) were obtained using the following:

$$aoc_x = \begin{cases} ao_{th}, & x_i > ao_{th} \\ 0, & x_i < ao_{th} \end{cases},$$
$$vc_x = x - aoc_x . \quad (2)$$

2.2.2 Step 2: Smoothing

The team quantized the data into power of discrete values in multiple of Δ_x to obtain the quantized variable component of power (qvc_x):

$$qvc_x = \Delta_x * floor \left[\frac{vc_x}{\Delta_x} + \frac{1}{2} \right]. \quad (3)$$

In preprocessing, the variable component of the power was quantized with a quantization step of 0.3 kW. Then, a median smoothing was performed on qvc_x to preserve the edge during any event while removing the transient portion of event detection.

$$ms - qvc_x = median \left\{ qvc_x \left[i - \frac{w_{ms}}{2} \right], qvc_x \left[i - \frac{w_{ms}}{2} + 1 \right], \dots, qvc_x \left[i + \frac{w_{ms}}{2} + 1 \right] \right\}, \quad (4)$$

where $ms - qvc_x$ is the median smoothed qvc_x .

Figure 1 shows an example of the raw active power signal and the preprocessed data. The figure shows that that data after preprocessing detected the edges of a power change while removing the transient portion of event detection.

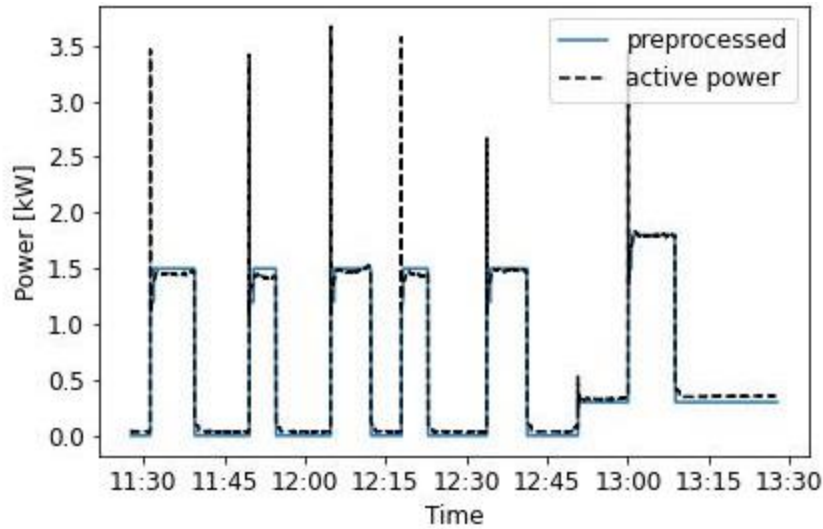


Figure 1. Time series of the raw active power signal and preprocessed data.

2.2.3 Step 3: Event Detection

Next, using the preprocessed data, the difference was measured between the consecutive element, and if the difference was not zero, then the change in power was labeled as an event. Because of the

quantization of data, the power change was in multiples of Δ_x . If the difference of the i^{th} element of the preprocessed data from $(i+1)^{\text{th}}$ element was positive (i.e., power had an increasing trend), then it was labeled as a start event, and if the difference was negative (i.e., power had a decreasing trend), then it was labeled as a stop event. Next, all the start events were paired with the next first stop event within the next 7,200 s with the same power change. An example of an event detected for a corresponding mains electrical signal is shown in Figure 2. The figure shows a start event (positive impulse) and stop event (negative impulse) corresponding to an increase and decrease in electrical power, respectively.

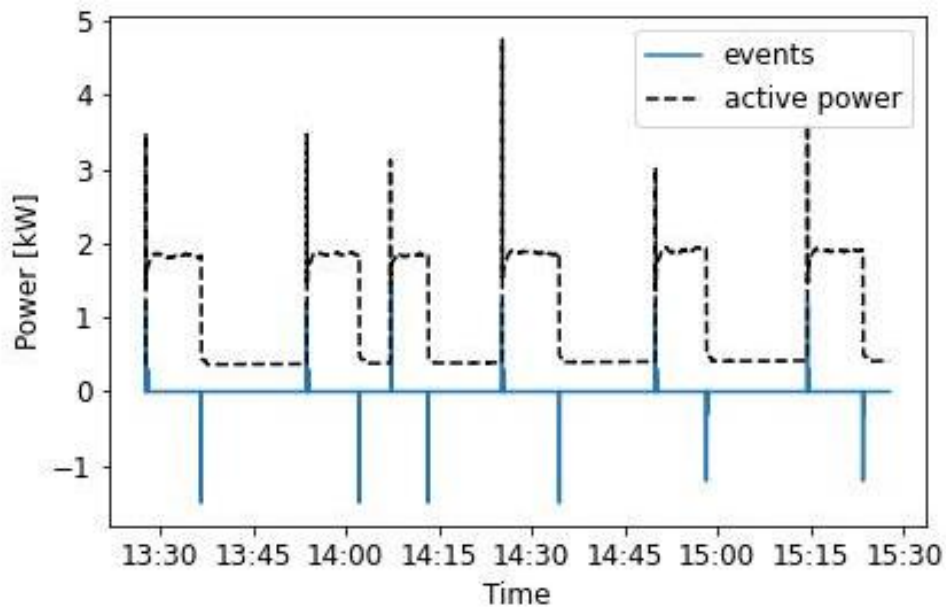


Figure 2. Time series of raw active power and events detected using preprocessed data.

2.3 EVENT CLASSIFICATION

The team used two methods for event classification of detected events. The first was an unsupervised method using k-means clustering of the active power signal during an appliance start event. The second was an RBC method that used rules formulated based on active and reactive power of individual appliances during different start events. Thus, the second approach used a supervised method.

2.3.1 K-Means Clustering

The team used k-means clustering to group the events observed from event detection into different categories. The clustering was done separately for the start events with a couple of iterations based on observations made from clustering.

k-means clustering iteration 1: A window of mains active power data 30 s before and 30 s after the occurrence of an event was first chosen. The reason for this selection was that event detection was performed after median filtering with a filter width of 30 s. Then, the data in this window were scaled in the range of 0 to 1. This scaling was performed so that the clustering occurred based on the power profile during the start event if the power of the different appliances of same category varied (e.g., a dryer with different rated power values). Five clusters were selected based on the elbow method (Kodinariya and Makwana 2013) using a plot of inertia as a function of the number of clusters (Figure 3). The clusters were created based on the dynamic time warping distance between the time series of the window. Figure 4 shows the results of the clustering. There are occurrences in clusters 0, 1, and 3 where the peaks of different elements of the clusters have similar shapes but also time lag. The second iteration of k-means clustering was performed to prevent this time lag.

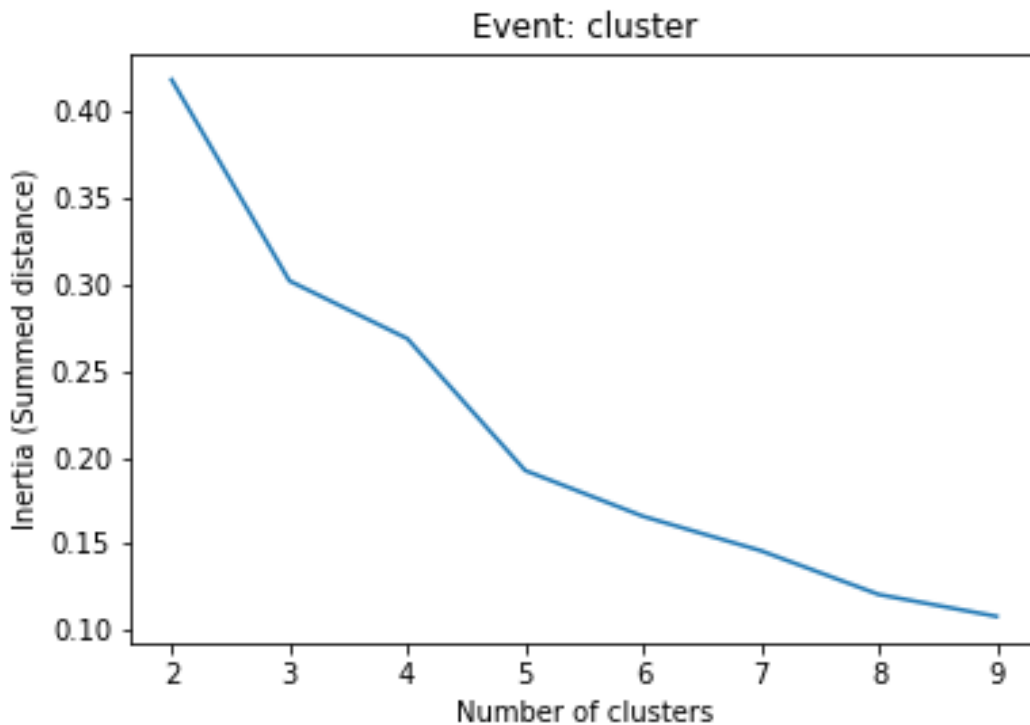


Figure 3. Plot of number of clusters vs. inertia.

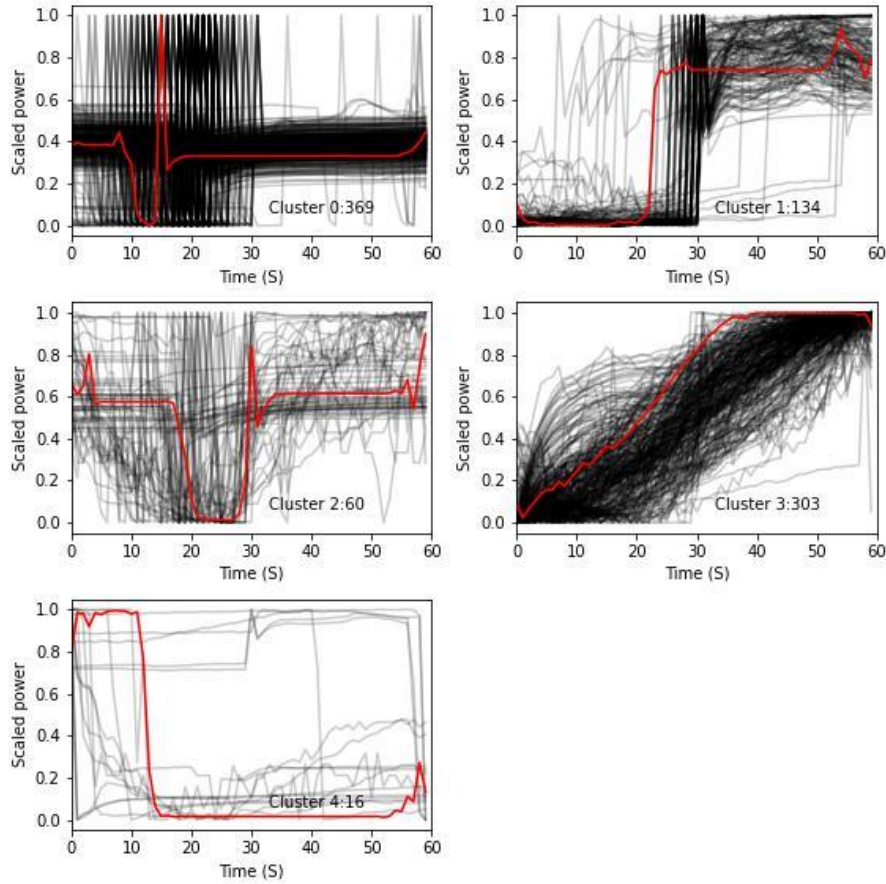


Figure 4. Clustering of equipment start events: iteration 1.

k-means clustering iteration 2: In this iteration, like in iteration 1, a window of mains active power data 30 s before and 30 s after the occurrence of event was chosen. Before normalizing the data, in this window, the location where the maximum power lies were chosen. After obtaining the point with maximum power, a window of 15 s before and 15 s after the maximum power was selected and scaled in the range of 0 to 1. Then, clustering was performed for the 31 s interval time series centered at its maximum power. After centering, five clusters were chosen based on the elbow method, similar to iteration 1. The results of *k-means* clustering after centering are shown in Figure 5. Each of these cluster shows more distinctive trends compared with the clusters in Figure 4. The red lines in each of the cluster represents the cluster center. In the figure, the Cluster 0 center starts around 0.5 and increases to 1 after a dip just before the peak and again becomes steady around 0.5. Cluster 1 center has steady power near 1 for most of the time period which dips down at the end of the window. Cluster 2 center mainly starts are relatively high power slowly increasing to 1 and has a smooth decline in power after the peak. Cluster 3 center rises from ~0 to 1 at the center of the window and then declines to a value ~0.7 at the end of the

window. Cluster 4 center starts from ~0 and remains such until the peak which dips after the peak and then becomes steady to ~0.7.

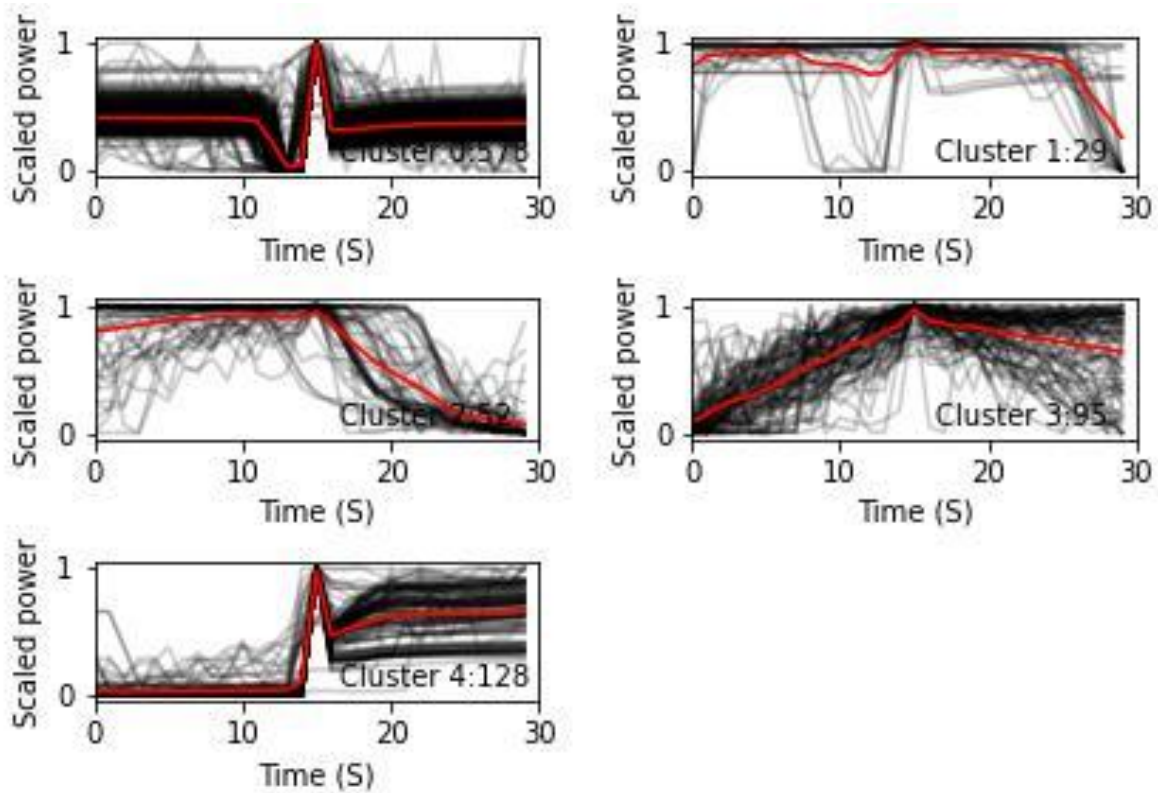


Figure 5. Clustering of equipment start events: iteration 2.

Clustering results check: The clusters created using the second iteration of k-means clustering show distinctive patterns but do not provide information on whether each of the clusters is a representation of the start of one or multiple appliances. Furthermore, knowing which appliance's startup is represented by the cluster would be valuable. To obtain this information, the power data collected for individual appliances were used to check if the appliance had a startup event when the event was detected using mains power data. The individual appliances were assumed to have a start event if their power increased by 0.3 kW within the time window when the start event occurred. Table 1 describes the different appliances with start events when a startup event was detected in the mains power data. The table indicates that a single cluster can have a startup event from multiple appliances clustered. For example, the HPWH startup appears to be present in all clusters.

Table 1. Appliance that had start event when a start event was detected in mains

Appliance	Cluster				
	0	1	2	3	4
Unknown	2	6	11	27	5
HPWH	12	18	41	67	88
HVAC_OD	154	2	0	0	11
HVAC_OD + HPWH	406	3	0	1	22
HVAC_OD + HVAC_ID	1	0	0	0	0
HVAC_OD + HPWH + Fridge	0	0	0	0	2
HVAC_OD + HVAC_ID + HPWH	3	0	0	0	0

2.3.2 RBC

Rules formulation: For using an RBC, the active power of the individual appliance was first used to detect events for each appliance. The appliance power cycle was considered between the period when the active power of the appliance went above the threshold of 0.3 kW until the period it went below that threshold. To detect the start event of the appliance, for each cycle, the team only considered the first 120 s of data to extract the features to use to formulate the RBC. After obtaining the appliance cycle for 120 s, the reactive power of the appliance was also obtained for the same time frame. The active and reactive power were assumed to be transient until the first 20 s, assuming all the power surge occurred during this interval, and then the appliance was assumed to work at normal power or steady-state power for the next 100 s. Following this assumption, polygon boundaries were formed for each of the appliances using the following for both active and reactive power:

- x_1 is 20th percentiles of the list of 20th percentiles of steady-state power values for each cycle
- x_2 is 80th percentiles of the list of 80th percentiles of steady-state power values for each cycle
- y_1 is 5th percentiles of the list of 95th percentiles transient power of each cycle
- y_2 is 95th percentiles of the list of 95th percentiles transient power of each cycle

For steady-state power, the team took the list of 20th percentile and 80th percentile values to examine the median steady-state power value. For transient power, the team only took 95th percentile values and found the 5th and 95th percentile of the list of 95th percentile because to examine the approximately maximum value during the power spike. The bounding boxes formed for different appliances are shown

in Figure 6. The bounding boxes were obtained to use them to create a rule for classifying the different startup events. If the median of steady-state power and 95th percentile value for transient power of the cycle of each appliance is used as x and y co-ordinates respectively, the point should lie inside or nearby their respective bounding boxes. One of the challenges here is to distinguish the events that fall in the region where the bounding boxes for two of the appliances overlap.

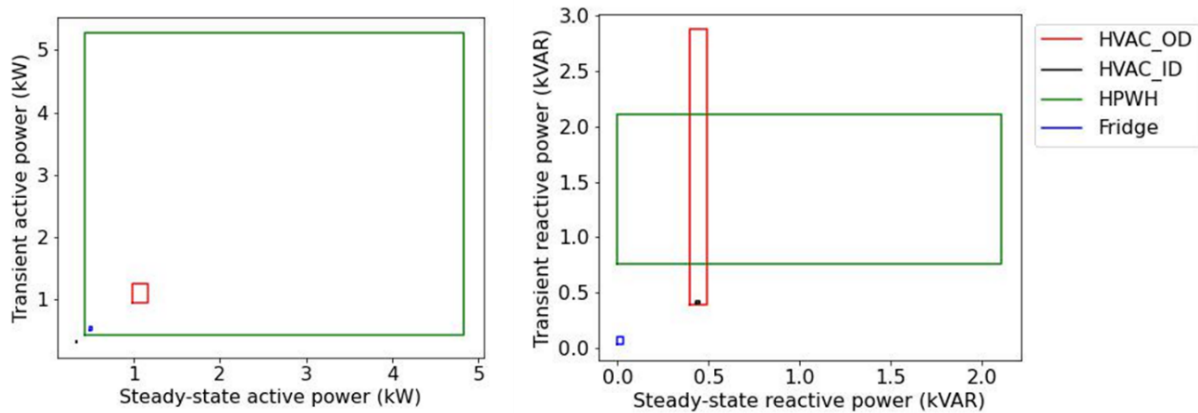


Figure 6. Bounding boxes for classification of different appliances.

Figure 7 shows the bounding boxes with scatter plots of the median for the steady-state portion and the 95th percentile transient power for each cycle of individual appliances. Here, the median and the 95th percentile were obtained from the individual power of the appliances. Figure 7 shows that for both active and reactive steady-state power median values can go out of the range in the x -axis, and 95th percentile transient power values can also go out of the range in the y -axis. This finding poses another problem for the assignment of the event data that fall outside of all the bounding boxes or some event data that fall inside multiple bounding boxes. To address this issue, the following method was used for the assignment of an event to the bounding box:

1. If an event data point was outside of all bounding boxes, then the minimum distance of the event data from each bounding box was calculated. The event was then assigned to the bounding box from which the distance for event data was smallest.
2. If an event data fell in only one bounding box, then the event corresponded to that bounding box.
3. If an event data was inside multiple bounding boxes, then the distance between the event data and centers of bounding boxes were calculated. The event was then assigned to the bounding box whose center was closest to the event data.

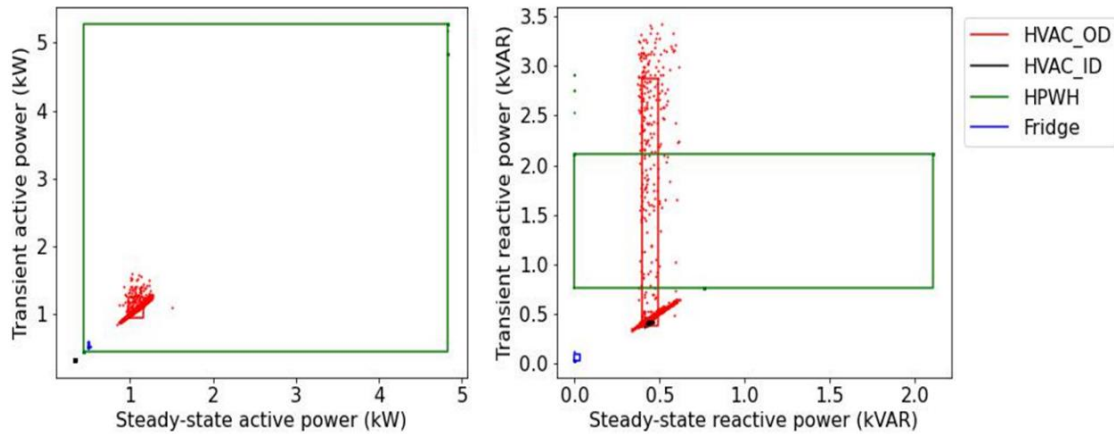


Figure 7. Bounding boxes for classification with scatter plot of transient-state 95th percentile power against steady-state median values obtained from individual power data of appliances.

Rules evaluation: Next, a check was performed to identify the appliance where the actual start event occurred at the time when the event was detected in the mains data using the methods discussed in Section 2.2. Here, since the actual transient and steady-state power is important, the power during the period before which cycle started was subtracted from the total mains power. The cycle thus detected was then used to calculate the median steady-state power and transient-state 95th percentile power for both active and reactive power, which was then used to classify the events as shown in Figure 8. Figure 8 shows that the scatter of the event and its classification is different from that in Figure 7, where the data from actual events obtained from individual data of the appliances were plotted.

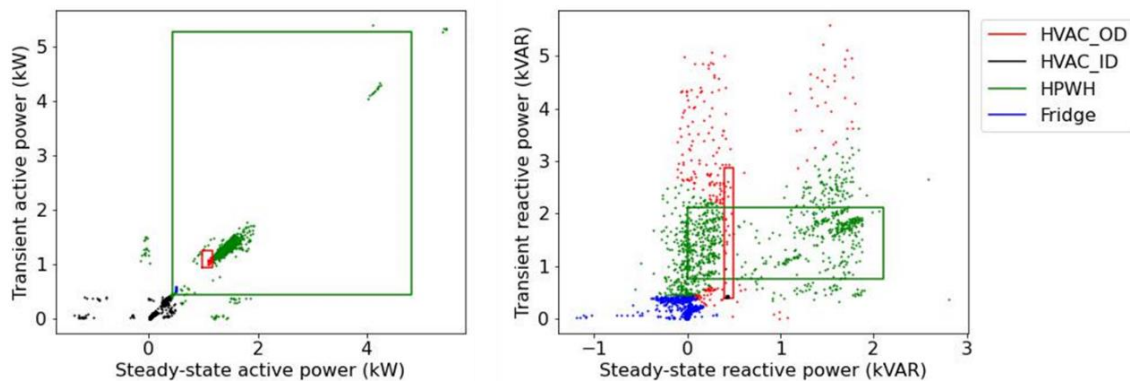


Figure 8. Bounding boxes for classification with scatter plots of transient-state 95th percentile power against steady-state median power obtained from disaggregation of mains electricity.

Next, a check was done for the appliance detected using active power and reactive power using the individual measured data as ground truth. Here, a check was done whenever an event was detected from

the mains electricity by taking a snippet of 30 s of individual appliance power around that event. Then, a maximum increase in electricity in that snippet was found by calculating the range from the start of the snippet until the location of maximum power occurrence. Cross-tables between the events detected from individual appliance power data and using RBC are provided in Table 2 and

Table 3. The tables provide the frequency of each appliance in the rows detected as appliances in each column. For example, in Table 2, the number 3 in the first cell of the cross-table represents the number of events when the fridge start event was detected as an HPWH start event.

Table 2. Cross-table of classification of appliances using RBC using active power vs. event detected using individual appliance power

		Detected using RBC (active power)				
		Fridge	HPWH	HVAC_ID	HVAC_OD	Unknown
Individual appliances	Fridge	0	3	1	0	0
	HPWH	0	1161	584	25	0
	HVAC_ID	0	0	0	0	0
	HVAC_OD	0	104	40	5	0
	Unknown	0	10	5	1	0

Table 3. Cross-table of classification of appliances using RBC using reactive power vs. event detected using individual appliance power

		Detected using RBC (reactive power)				
		Fridge	HPWH	HVAC_ID	HVAC_OD	Unknown
Individual appliances	Fridge	2	1	0	1	0
	HPWH	614	940	1	215	0
	HVAC_ID	0	0	0	0	0
	HVAC_OD	65	67	0	17	0
	Unknown	6	10	0	0	0

Based on the results in Table 2 and

Table 3, the true positive (TP), false positive (FP), true negative (TN), and false negative (FN) values were calculated for each of the appliances. The definition of TP, FP, TN and FN are as follows, where the

event detected from individual appliances is the actual event, and the event using RBC is the predicted event:

- TP: actual event, yes; predicted event, yes
- TN: actual event, no; predicted event, no
- FP: actual event, no; predicted event, yes
- FN: actual event, yes; predicted event, no

Based on these values, the recall, precision, accuracy, and F1-score were also calculated for individual appliances using Eqs. (5)–(8). The results from the calculations of these metrics for classification using active power data and reactive power data are provided in Table 4 and Table 5, respectively. The “N/A” in the tables is present for recall and/or precision due to division by zero and corresponding F1-score when either recall or precision in N/A was also N/A.

$$Recall = \frac{TP}{TP+FN} \quad (5)$$

$$Precision = \frac{TP}{TP+FP} \quad (6)$$

$$Accuracy = \frac{TP+TN}{TP+FP+TN+FN} \quad (7)$$

$$F1 - score = 2 * \left(\frac{Precision * Recall}{Precision + Recall} \right) \quad (8)$$

In Table 4 and Table 5, recall, which represents the fraction of actual events for an appliance, correctly predicted range from 0.03 to 0.66 (excluding the unknown category because this category was not used during prediction of an event class). Precision, which represents the fraction of events that are predicted as an appliance being the actual event for the same appliance and not other appliances, was greater than 0.9 for the HPWH. This indicates that more than 90% of the events classified as HPWH were actually events due to operation of the HPWH. However, this metric was only 0.16 using active power data and 0.07 using reactive power data for HVAC_OD. Table 4 and Table 5 shows that the highest F1-score was for the HPWH while using both active power (0.77) and reactive power (0.67). For all other appliances, the F1-score was either N/A or below 0.1. This indicates that except for the HPWH, the classification of events from the use of the RBC needs significant improvement.

Table 4. Appliance classification metrics using active power

	TP	FP	FN	TN	Recall	Precision	Accuracy	F1-score
Fridge	0	0	4	1,935	0	N/A	1	N/A
HPWH	1,161	117	609	52	0.66	0.91	0.63	0.77
HVAC_ID	0	630	0	1,309	N/A	0	0.68	N/A
HVAC_OD	5	26	144	1,764	0.03	0.16	0.91	0.05
Unknown	0	0	16	1,923	0	N/A	0.99	N/A

Table 5. Appliance classification metrics using reactive power

	TP	FP	FN	TN	Recall	Precision	Accuracy	F1-score
Fridge	2	685	2	1,250	0.5	0	0.65	0
HPWH	940	78	830	91	0.53	0.92	0.53	0.67
HVAC_ID	0	1	0	1,938	N/A	0	1	N/A
HVAC_OD	17	216	132	1,574	0.11	0.07	0.82	0.09
Unknown	0	0	16	1,923	0	N/A	0.99	N/A

3. CONCLUSIONS

NILM was performed with data collected from Oak Ridge National Laboratory’s Yarnell Station research house for approximately 1.5 month. An event detection algorithm was used to find appliance start-up event, followed by event classification. Event classification was performed using two methods—first, an unsupervised approach with k-means clustering, and second, a supervised approach using RBC. From clustering, the events from a single appliance were present in multiple clusters, so the groups could not be categorized as a single appliance. Using RBC, the events were classified into different appliances and evaluated using the power data for individual appliances. The results demonstrate that the classification had an F1-score of 0.77 using active power data of the HPWH, but for all the other appliances, the value was very low. The method used for NILM in this project could be enhanced or other alternative methods could be used to increase the accuracy of NILM.

4. REFERENCES

- Faustine, Anthony, Nerey Henry Mvungi, Shubi Kaijage, and Kisangiri Michael. 2017. “A Survey on Non-Intrusive Load Monitoring Methodies and Techniques for Energy Disaggregation Problem.” *ArXiv*.
- Filip, Adrian. 2011. “Blued: A Fully Labeled Public Dataset for Event-Based Nonintrusive Load

- Monitoring Research.” In *2nd Workshop on Data Mining Applications in Sustainability (SustKDD)*. Vol. 2012.
- Gelazanskas, Linas, and Kelum A.A. Gamage. 2014. “Demand Side Management in Smart Grid: A Review and Proposals for Future Direction.” *Sustainable Cities and Society* 11: 22–30. <https://doi.org/10.1016/j.scs.2013.11.001>.
- Hart, George W. 1992. “Nonintrusive Appliance Load Monitoring.” *Proceedings of the IEEE* 80 (12): 1870–91. <https://doi.org/10.1109/5.192069>.
- Hosseini, Sayed Saeed, Kodjo Agbossou, Souso Kelouwani, and Alben Cardenas. 2017. “Non-Intrusive Load Monitoring through Home Energy Management Systems: A Comprehensive Review.” *Renewable and Sustainable Energy Reviews* 79 (April): 1266–74. <https://doi.org/10.1016/j.rser.2017.05.096>.
- Kodinariya, Trupti M, and Prashant R Makwana. 2013. “Review on Determining Number of Cluster in K-Means Clustering.” *International Journal* 1 (6): 90–95.
- Langevin, Jared, Chioke B. Harris, Aven Satre-Meloy, Handi Chandra-Putra, Andrew Speake, Elaina Present, Rajendra Adhikari, Eric J.H. Wilson, and Andrew J. Satchwell. 2021. “US Building Energy Efficiency and Flexibility as an Electric Grid Resource.” *Joule* 5 (8): 2102–28. <https://doi.org/10.1016/j.joule.2021.06.002>.
- Le, Thi Thu Huong, and Howon Kim. 2018. “Non-Intrusive Load Monitoring Based on Novel Transient Signal in Household Appliances with Low Sampling Rate.” *Energies* 11 (12). <https://doi.org/10.3390/en11123409>.
- Parson, Oliver, Grant Fisher, April Hersey, Nipun Batra, Jack Kelly, Amarjeet Singh, William Knottenbelt, and Alex Rogers. 2016. “Dataport and NILMTK: A Building Data Set Designed for Non-Intrusive Load Monitoring.” *2015 IEEE Global Conference on Signal and Information Processing, GlobalSIP 2015*, 210–14. <https://doi.org/10.1109/GlobalSIP.2015.7418187>.
- Pattem, Sundeep. 2012. “Unsupervised Disaggregation for Non-Intrusive Load Monitoring.” *Proceedings - 2012 11th International Conference on Machine Learning and Applications, ICMLA 2012* 2: 515–20. <https://doi.org/10.1109/ICMLA.2012.249>.
- Ruano, Antonio, Alvaro Hernandez, Jesus Ureña, Maria Ruano, and Juan Garcia. 2019. “NILM Techniques for Intelligent Home Energy Management and Ambient Assisted Living: A Review.” *Energies* 12 (11): 1–29. <https://doi.org/10.3390/en12112203>.
- Siano, Pierluigi. 2014. “Demand Response and Smart Grids - A Survey.” *Renewable and Sustainable*

Energy Reviews 30: 461–78. <https://doi.org/10.1016/j.rser.2013.10.022>.

United States Department of State. 2021. “The Long-Term Strategy of the United States: Pathways to Net-Zero Greenhouse Gas Emissions by 2050.” *United States Department of State and the United States Executive Office of the President*, no. November: 1–63. <https://www.whitehouse.gov/wp-content/uploads/2021/10/US-Long-Term-Strategy.pdf>.

“US Energy Information Administration.” 2019. US Energy Information Administration. 2019.